Hindawi
Geofluids
Volume 2021, Article ID 9906500, 18 pages
https://doi.org/10.1155/2021/9906500

Research Article

Quantitative Characterization of Pore Space for the Occurrence of Continental Shale Oil in Lithofacies of Different Types: Middle Jurassic Lianggaoshan Formation in Southeastern Sichuan Basin of the Upper Yangtze Area

Xiangfeng Wei,[1,2] Kun Zhang,[3,4,5,6] Qianwen Li,[1,7] Dongfeng Hu,[2] Zhihong Wei,[2] Ruobing Liu,[2] Zhujiang Liu,[2] and Jiayi Liu[1,7]

[1]*State Key Laboratory of Shale Oil and Gas Enrichment Mechanisms and Effective Development, Beijing 100083, China*
[2]*Sinopec Exploration Company, Chengdu 610041, China*
[3]*School of Geoscience and Technology, Southwest Petroleum University, Chengdu 610500, China*
[4]*State Key Laboratory of Oil and Gas Reservoir Geology and Exploitation, Southwest Petroleum University, Chengdu 610500, China*
[5]*Key Laboratory of Tectonics and Petroleum Resources (China University of Geosciences), Ministry of Education, Wuhan 430074, China*
[6]*Energy and Geoscience Institute, University of Utah, Salt Lake City, Utah 84108, USA*
[7]*Sinopec Petroleum Exploration and Production Research Institute, Beijing 100083, China*

Correspondence should be addressed to Kun Zhang; shandongzhangkun@126.com

Received 25 August 2021; Accepted 18 October 2021; Published 27 October 2021

Academic Editor: Amer Syed

In addition to marine and marine-continental transitional strata, the continental ones are also widely distributed in various oil and gas-bearing basins in China. The continental shale generally provides favorable material bases for hydrocarbon generation, such as wide distribution, large thickness, multiple series of strata, high TOC content, nice organic matter type, and moderate thermal evolution. Part of such shale contains shale oil, but the pore space characteristics for the occurrence of this oil are not thoroughly studied. In order to accurately and quantitatively characterize the pore space where the continental shale oil in different types of lithofacies occurs, we sampled the rock cores from the Middle Jurassic Lianggaoshan Formation in the southeastern Sichuan Basin of the Upper Yangtze Area. The TOC content and mineral composition were analyzed, and we also carried out experiments on CO_2 and N_2 adsorptions, high-pressure mercury injection, and wash oil. Results show significant differences in pore space characteristics for the occurrence of shale oil in different types of lithofacies. In organic-rich mixed and clayey mudstones with the highest TOC content, the free shale oil, occupying the largest reservoir space, mainly occurs in macropores and mesopores, and the adsorbed shale oil, occupying the largest reservoir space, mainly occurs in mesopores. In the organic-bearing clayey mudstone, which has a higher TOC content, the free shale oil takes a larger reservoir space and mainly occurs in macropores, followed by mesopores, and the absorbed one, occupying a larger reservoir space, mostly occurs in micropores and then the mesopores. The organic-bearing mixed mudstone has a moderate TOC content, in which the free shale oil occupies a smaller reservoir space and primarily occurs in mesopores, followed by macropores, and the absorbed one, which takes a larger reservoir space, all occurs in mesopores. In the fine sandstone, the free shale oil occupies a smaller reservoir space and primarily occurs in mesopores, while the absorbed one occupies a smaller reservoir space and all occurs in mesopores.

1. Introduction

The change in geological concepts and the achievements made in horizontal well drilling and fracturing technologies in recent years brought a remarkable breakthrough in China's exploration of marine shale gas, and various shale gas fields have been successively built at Jiaoshiba, Weiyuan, Changning, Fushun-Yongchuan, Zhaotong, Luzhou, etc. [1–7] Besides, continental strata are also widely distributed in China's oil and gas-bearing basins, including Sichuan, Junggar, and Bohai Bay Basins. In particular, the continental shale in Jianghan Basin is featured with wide distribution, large thickness, multiple series of strata, high TOC content, moderate thermal evolution, and good kerogen type. Therefore, oil companies, such as PetroChina and the Sinopec Group, have attached great importance to the geological research on continental shale oil and gas and have planned to exert more efforts in exploration during China's "14th Five-Year Plan" [8–14].

Since shale pores are major reservoir spaces and seepage channels of shale oil, it is urgent to study the pore space characteristics for shale oil occurrence. Li et al. [15] argued that since shale oil mainly occurs in shale pores, research into the pore structure characteristics is the key to understand the mechanism of shale oil accumulation. In the lower third member of the continental Shahejie Formation in the Zhanhua Sag, shale micro-nanopore structure is qualitatively and quantitatively characterized with FE-SEM, CO_2 adsorption, N_2 adsorption, and high-pressure mercury injection [15]. Taking the continental shale of Zhanhua Sag in the Jiyang Depression of the Bohai Bay Basin as the examples, Su et al. used microscope and nuclear magnetic resonance (NMR) to examine the hydrocarbon generation and expulsion of nitrogen adsorption, reservoir properties, and oil-gas bearing capacity of different shale lithofacies [16]. To reveal the effects of shale reservoir characteristics on the movability of shale oil and its action mechanism in the lower third member of the Shahejie Formation, Ning et al. selected samples with different features and analyzed them using N_2 adsorption, high-pressure mercury injection capillary pressure (MICP), nuclear magnetic resonance (NMR), high-speed centrifugation, and displacement image techniques [17].

In this work, the continental shale was sampled from the Middle Jurassic Lianggaoshan Formation in southeastern Sichuan Basin of the Upper Yangtze Area in South China, and the key TY1 exploration well was selected to study the characteristics of pore space where the continental shale oil in different types of lithofacies occurs (Figure 1). First, the shale lithofacies were classified by TOC content and mineral composition. Then, the shale samples collected from the same depth were divided into two groups. For one of them, the experiments on CO_2 and N_2 adsorptions and high-pressure mercury injection were conducted to characterize the distribution features of micropores, mesopores, and macropores, thus quantitatively characterizing the full-scale pore structure of these samples before extraction. For the other group, the shale oil was first extracted from samples by wash oil, and the above experiments were repeated to obtain the same kind of data. Finally, the data before and after extraction were compared to obtain the pore space characteristics.

2. Geological Settings

2.1. Tectonic Framework. The study area, located at the high-steep fault-fold zone of East Sichuan, is an arcuate tectonic belt composed of a series of arcuate mountains. It is bounded by the Huayingshan Fault Zone, is adjacent to the Central Sichuan Uplift in the west, and stretches eastwards to the Qiyueshan Fault Zone on the Sichuan-Hubei border. The structural lineament mainly develops in the direction of NNE, extends towards NEE, and finally converges in the north [18–20]. In this tectonic belt, mountains are formed by high-steep anticlines with Permian-Triassic cores and asymmetrical wings, of which the gentle wing generally shows a stratigraphic dip of 20°~30°, while the steep one shows a stratigraphic dip of 40°~70° or a vertically inverted stratum. Besides, the broad valleys between these mountains are formed by wide and gentle synclines, which are developed in the Jurassic period and show a typical partition style both in structure and landform [21–24].

2.2. Sedimentology and Stratigraphy. The studied area in the Lianggaoshan Formation is divided into three members, of which both the first and second ones can be further divided into upper and lower submembers [25–30]. Meanwhile, this formation develops a set of gray siltstone, silty shale, black gray-dark gray shale, and fine gray siltstone. Besides, the dark gray shale primarily deposits in the upper submember of the first member and the lower submember of the second member, which are the strata suitable for the development of organic-rich shale (Figure 2). The Lianggaoshan Formation undergoes a complete cycle of lake transgression and regression during the sedimentation. Thereinto, the first member of this formation has sufficient provenance supply at the early stage of sedimentation and then experiences the lake transgression. The second member, mainly developing the shallow and semideep lacustrine deposits, reaches the maximum flood surface in the early stage and later experiences the lake regression. It is a favorable facies belt for the development of organic-rich shale. The third member primarily develops the coarse clastic materials in the delta front. Moreover, the upper submember of the first member and the lower submember of the second member are major strata, in which the dark argillaceous shale is developed [31–34].

3. Samples, Experiments, and Data Sources

In this study, the shale was sampled from the Lianggaoshan Formation in the TY1 well according to 14 depths, with the sample number shown in Table 1. First, the shale lithofacies were classified by measuring the TOC content of samples at the same depth with a Sievers 860 TOC analyzer and by performing the X-ray diffraction analysis on whole rocks and minerals with a YST-I mineral analyzer. Then, the shale samples collected from the same depth were equally divided into two groups. For one group, the BSD-PM1/2

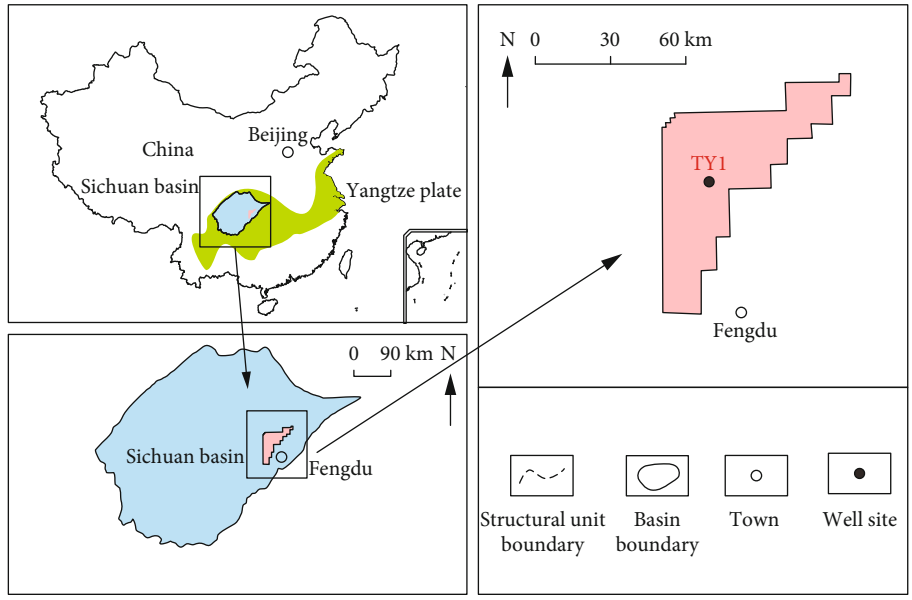

Figure 1: Locations of southeastern Sichuan Basin in South China and TY1 well site.

instrument was used for the CO_2 adsorption experiment to obtain the pore size distribution characteristics of micropores (<2 nm), the BSD-PS1/2/4 instrument was used for the N_2 adsorption experiment to obtain such characteristics of mesopores (2~50 nm), and the 3H-2000PS2 instrument was used for the high-pressure mercury injection experiment to obtain such characteristics of macropores (>50 nm). Then, the data about these three experiments were combined to determine the joint characterization for the full-scale pore structure of samples before the shale oil was extracted.

As for the other group, the DY-6 instrument was used for the wash oil experiment to extract the shale oil from samples at the same depth. Similarly, the CO_2 adsorption experiment was conducted with the BSD-PM1/2 instrument to obtain the pore size distribution characteristics of micropores (<2 nm), the N_2 adsorption experiment was conducted with BSD-PS1/2/4 instrument to obtain such characteristics of mesopores (2~50 nm), and the high-pressure mercury injection experiment was conducted with a 3H-2000PS2 instrument to obtain such characteristics of macropores (>50 nm). Then, the data about these three experiments were combined to determine the joint characterization for the full-scale pore structure of samples after the shale oil was extracted. Finally, the characterization results before and after extraction were compared to obtain the quantitative characterization of pore space for the occurrence of shale oil in different types of lithofacies.

4. Results and Discussion

4.1. Division of Shale Lithofacies. In previous studies, the shale lithofacies were divided based on the mineral composition and TOC content. (1) It is classified into 4 types according to the mineral composition: clayey shale (clay minerals ≥ 50%), calcareous shale (carbonate minerals ≥ 50), and mixed shale (siliceous, clay, and carbonate minerals < 50%) (Figure 3). (2) It is classified into 3 types according to the TOC content: organic-lean shale (TOC content = 0% ~ 1%), organic-bearing shale (TOC content = 1% ~ 2%), and organic-rich shale (TOC content ≥ 2%). When the two classification methods are integrated, there will be $3 \times 4 = 12$ types of lithofacies [35–42]. Table 1 shows different types of shale lithofacies divided based on the TOC content and mineral composition of 14 shale samples.

4.2. Pore Structure Characteristics for Different Types of Shale Lithofacies before and after the Extraction of Shale Oil. In the Lianggaoshan Formation, the pore volume and surface area provide the occurrence space for free and absorbed shale oils, respectively [43–45]. In this paper, the shale samples at the same depth were divided into two groups, one of which was analyzed to quantitatively characterize the full-scale pore size of samples containing the shale oil by characterizing the distribution features of micropores, mesopores, and macropores through experiments on CO_2 and N_2 adsorptions and high-pressure mercury injection, respectively [46–55].

For the other group, the wash oil was used to extract and remove the shale oil from sample pores at the same depth. Then similarly, the distribution features of micropores, mesopores, and macropores were characterized by experiments on CO_2 and N_2 adsorptions and high-pressure mercury injection, respectively, thus quantitatively characterizing the full-scale pore size of samples without shale oil [56–60], as shown in Figures 4 and 5.

4.2.1. Pore Volume Characteristics for the Occurrence of Shale Oil. The analysis on pore volume characteristics of rock reservoirs adopted the experimental data after the

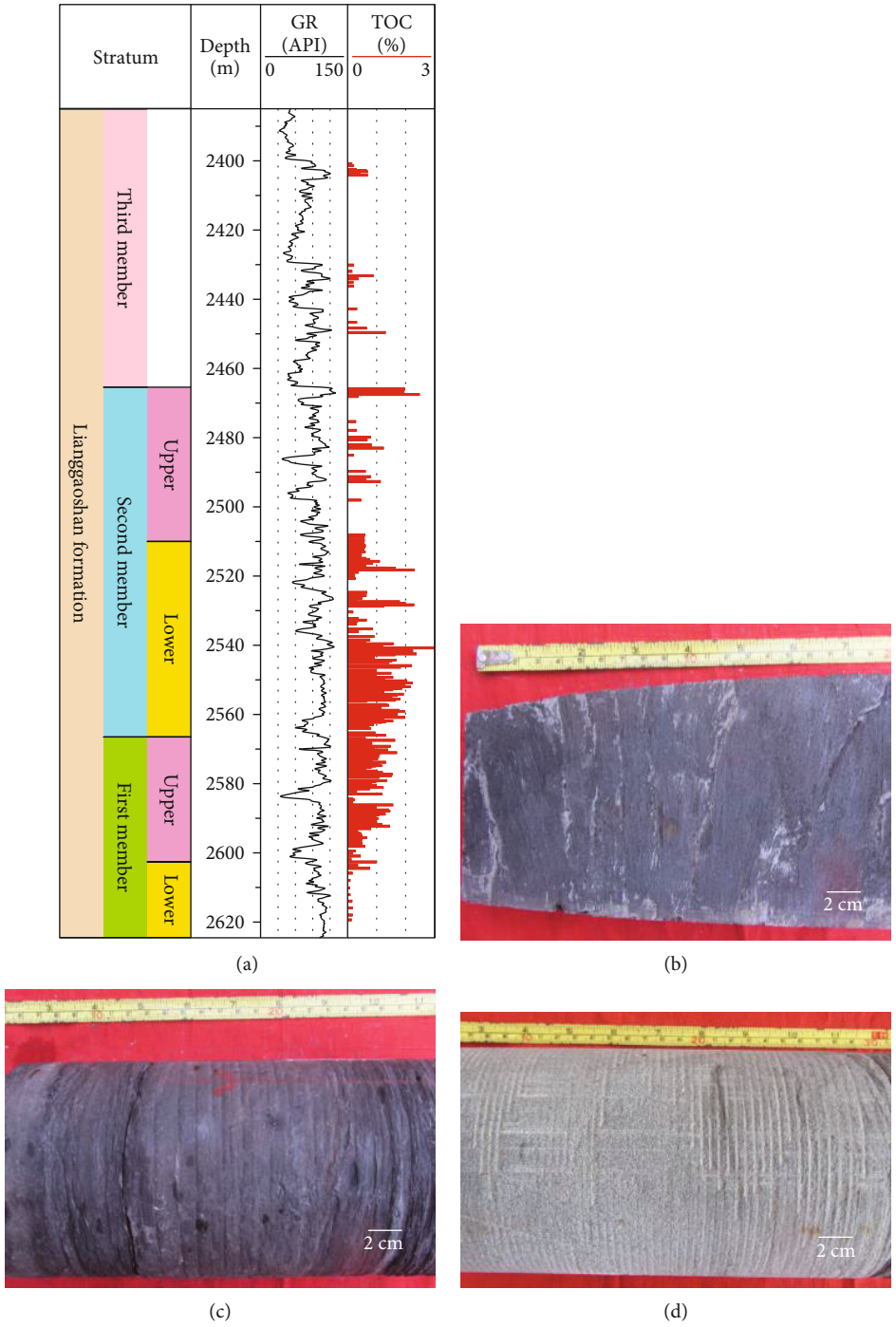

Figure 2: Column diagram and core photos of the Middle Jurassic Ranggosan Formation stratigraphy in well TY1. (a) Stratigraphic column diagram of the TY1 well; (b) dark gray shale of the upper subsection of the first section of the Ryanggosan Formation in TY1 well, 2579 m; (c) gray-black shale of the lower subsection of the second section of the Ryanggosan Formation in TY1 well, 2542 m; (d) gray fine sandstone of the third section of the Ryanggosan Formation in TY1 well, 2421 m. See Figure 1 for the well locations.

Table 1: Experimental sample depth, layer section, and petrographic classification.

Sample number	Depth (m)	Formation	Lithofacies
1	2403.93	The third member of Lianggaoshan Formation	Organic-bearing mixed shale
2	2466.7	Upper submember of the second member of Lianggaoshan Formation	Organic-rich clayey shale
3	2470.82	Upper submember of the second member of Lianggaoshan Formation	Fine sandstone
4	2515.82	Lower submember of the second member of Lianggaoshan Formation	Organic-bearing clayey shale
5	2527.04	Lower submember of the second member of Lianggaoshan Formation	Organic-rich clayey shale
6	2540.45	Lower submember of the second member of Lianggaoshan Formation	Organic-rich clayey shale
7	2542.24	Lower submember of the second member of Lianggaoshan Formation	Organic-rich clayey shale
8	2547.35	Lower submember of the second member of Lianggaoshan Formation	Organic-rich mixed shale
9	2552.98	Lower submember of the second member of Lianggaoshan Formation	Organic-rich clayey shale
10	2555.65	Lower submember of the second member of Lianggaoshan Formation	Organic-rich clayey shale
11	2573.32	Upper submember of the first member of Lianggaoshan Formation	Organic-rich mixed shale
12	2576.98	Upper submember of the first member of Lianggaoshan Formation	Organic-bearing clayey shale
13	2579.45	Upper submember of the first member of Lianggaoshan Formation	Organic-bearing clayey shale
14	2589.7	Upper submember of the first member of Lianggaoshan Formation	Organic-bearing clayey shale

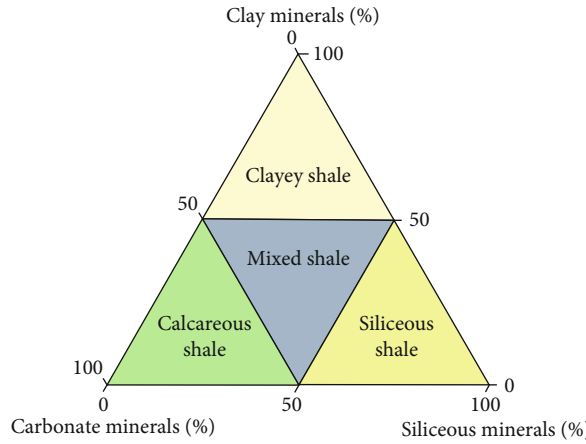

Figure 3: Shale petrographic diagram based on mineralogical composition.

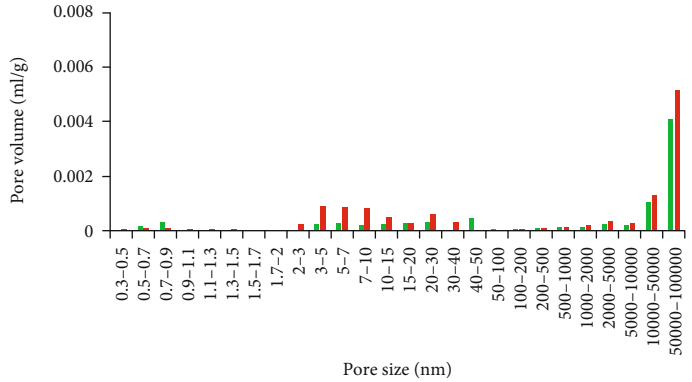

(a) 2403.93 m, organic-bearing mixed shale

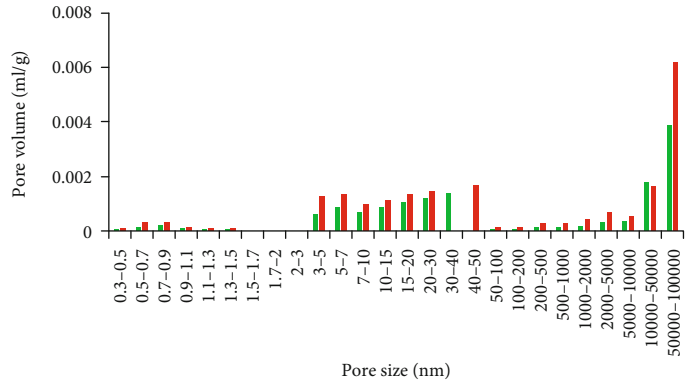

(b) 2466.7 m, organic-rich clayey shale

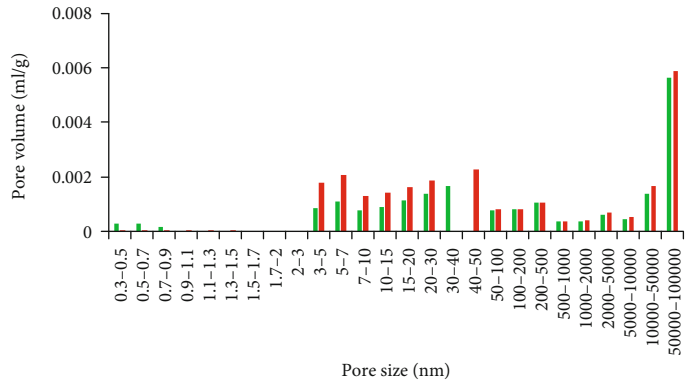

(c) 2470.82 m, fine sandstone

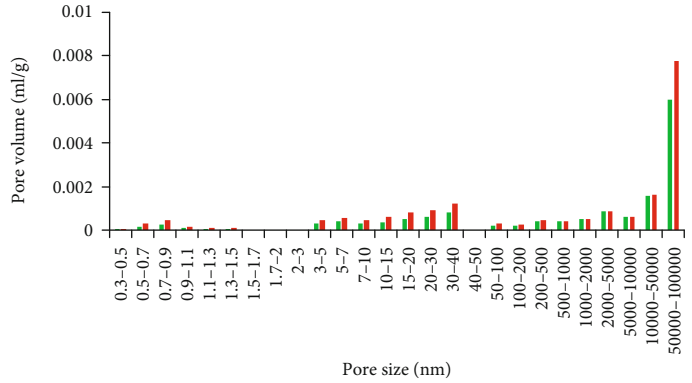

(d) 2515.82 m, organic-bearing clayey shale

Figure 4: Continued.

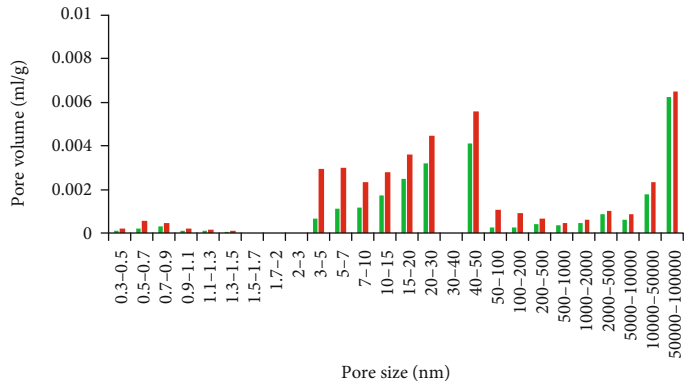

(e) 2527.04 m, organic-rich clayey shale

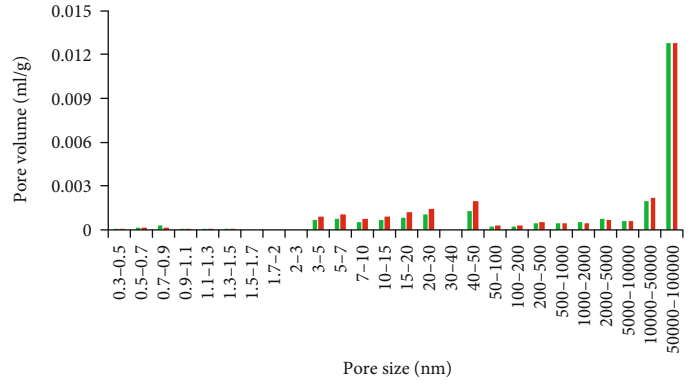

(f) 2540.45 m, organic-rich clayey shale

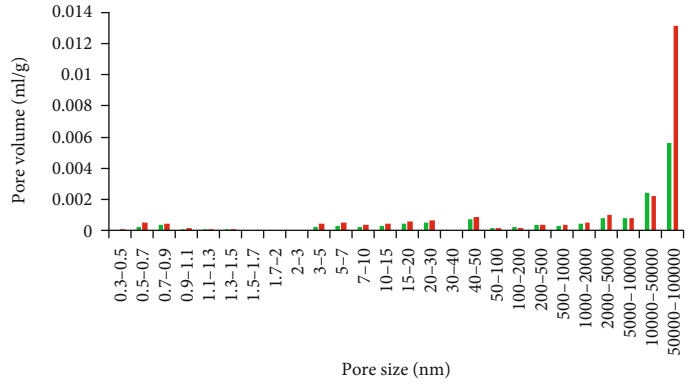

(g) 2542.24 m, organic-rich clayey shale

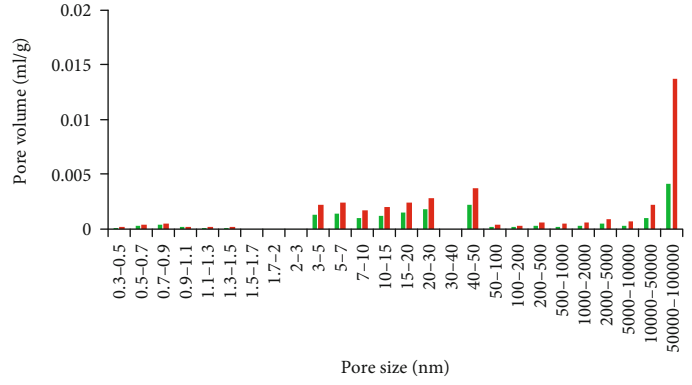

(h) 2547.35 m, organic-rich mixed shale

Figure 4: Continued.

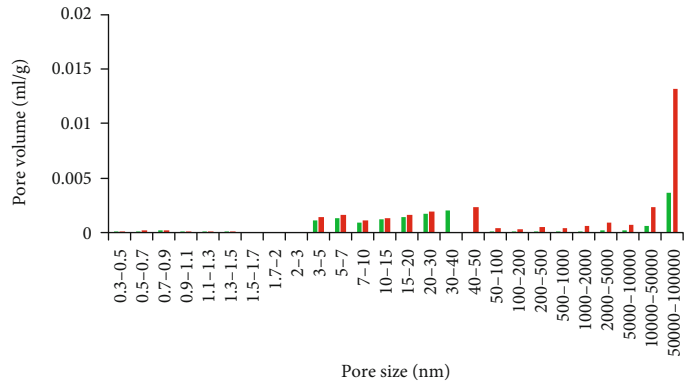

(i) 2552.98 m, organic-rich clayey shale

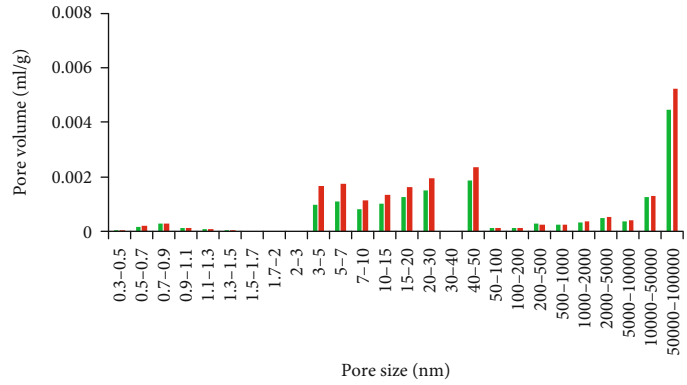

(j) 2555.65 m, organic-rich clayey shale

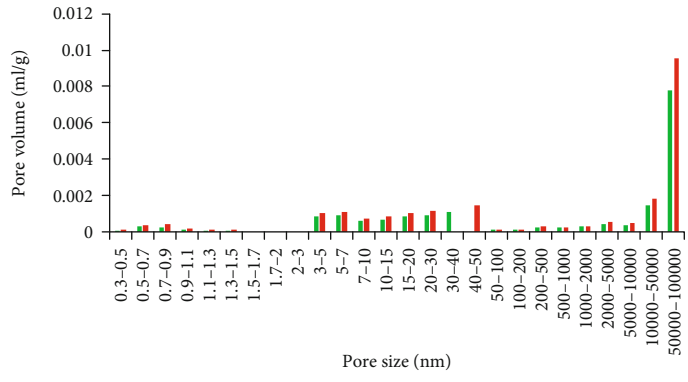

(k) 2573.32 m, organic-rich mixed shale

Figure 4: Continued.

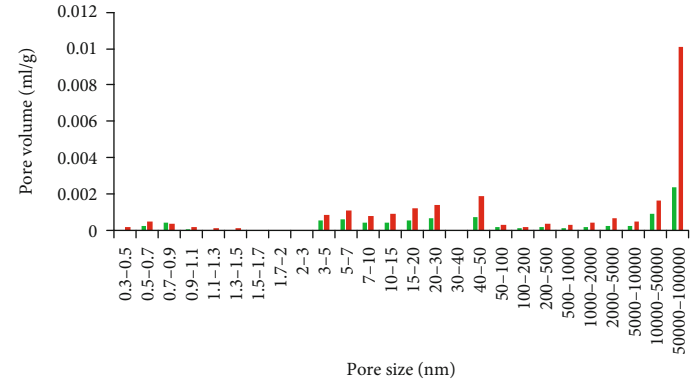

(l) 2576.98 m, organic-bearing clayey shale

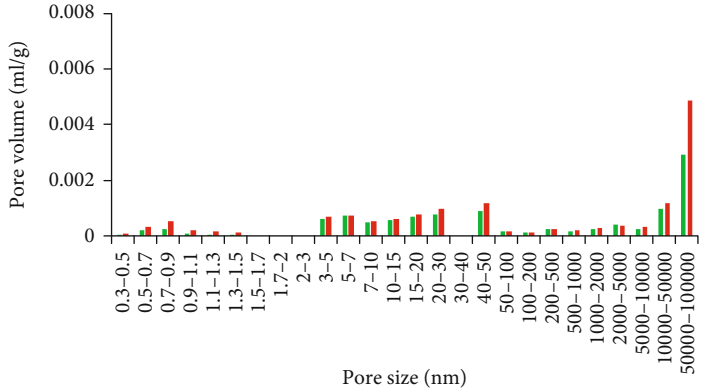

(m) 2579.45 m, organic-bearing clayey shale

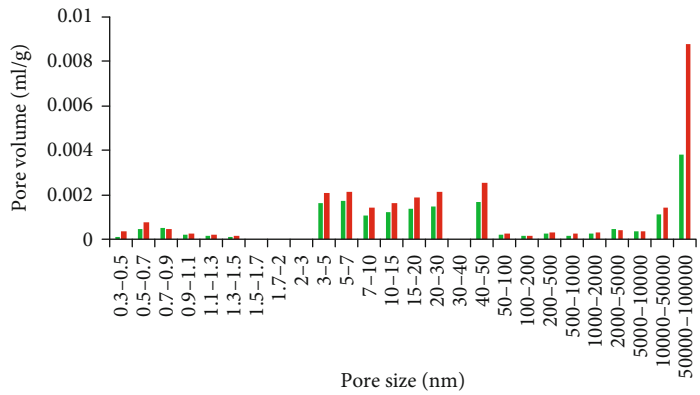

(n) 2589.7 m, organic-bearing clayey shale

Figure 4: Pore volume features based on the joint characterization for full-scale pore size of different shale samples in TY1 well. Green: pore volume data of shale samples before the extraction of shale oil; Red: pore volume data of shale samples after the extraction of shale oil.

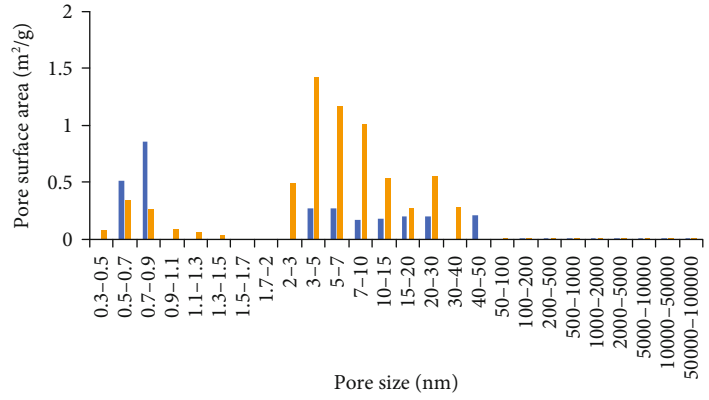

(a) 2403.93 m, organic-bearing mixed shale

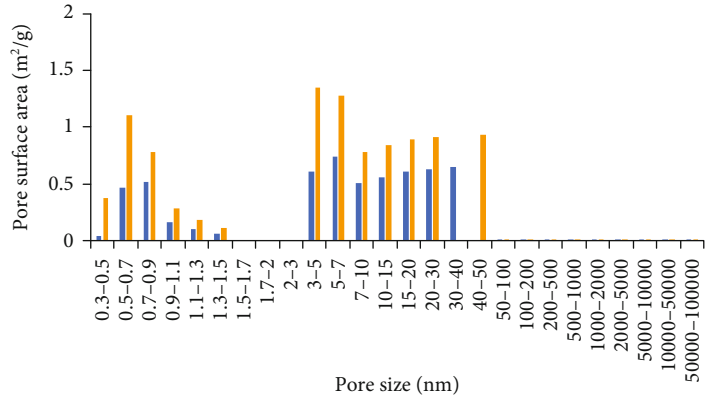

(b) 2466.7 m, organic-rich clayey shale

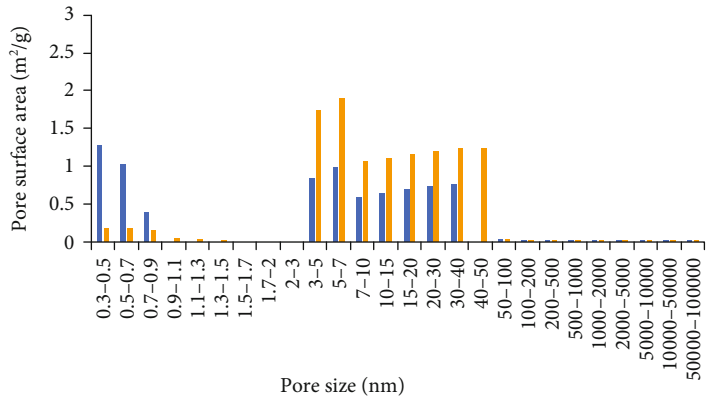

(c) 2470.82 m, fine sandstone

Figure 5: Continued.

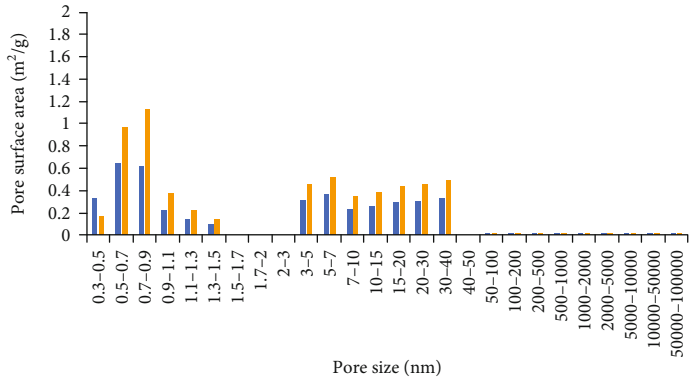

(d) 2515.82 m, organic-bearing clayey shale

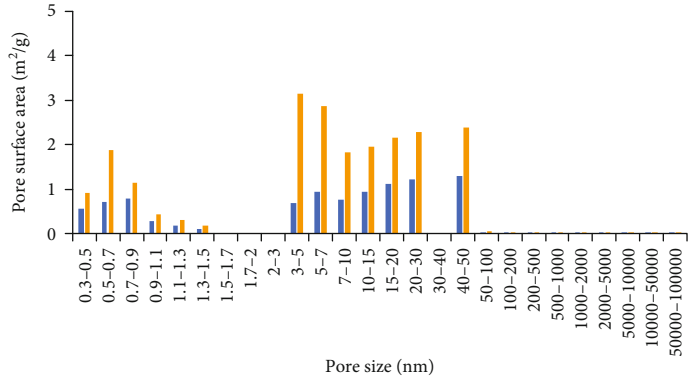

(e) 2527.04 m, organic-rich clayey shale

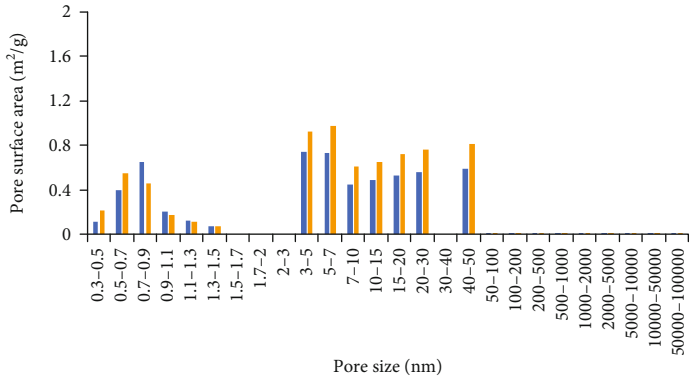

(f) 2540.45 m, organic-rich clayey shale

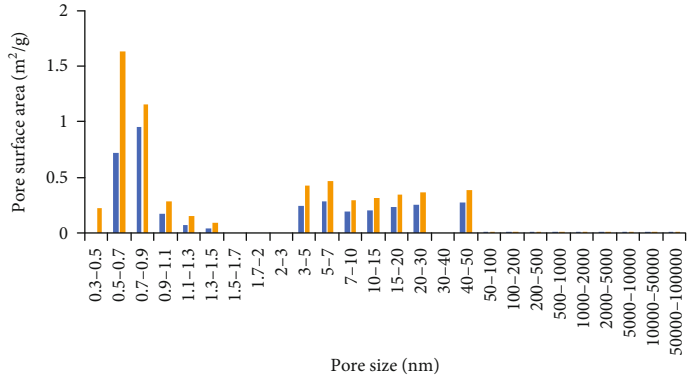

(g) 2542.24 m, organic-rich clayey shale

Figure 5: Continued.

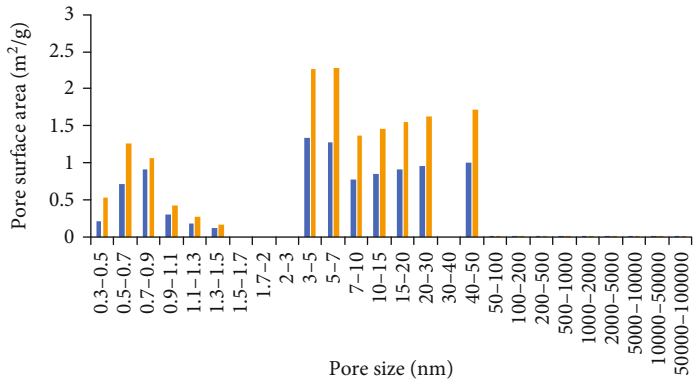

(h) 2547.35 m, organic-rich mixed shale

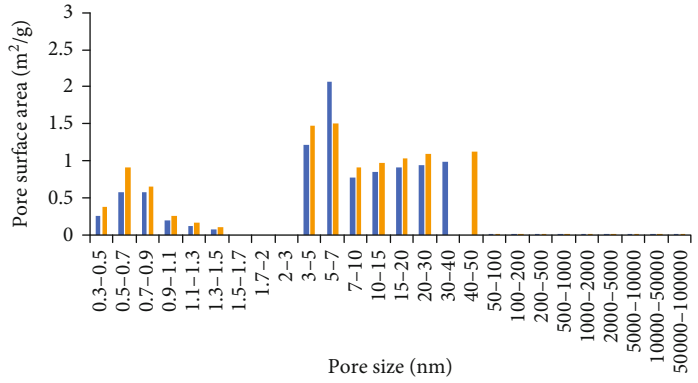

(i) 2552.98 m, organic-rich clayey shale

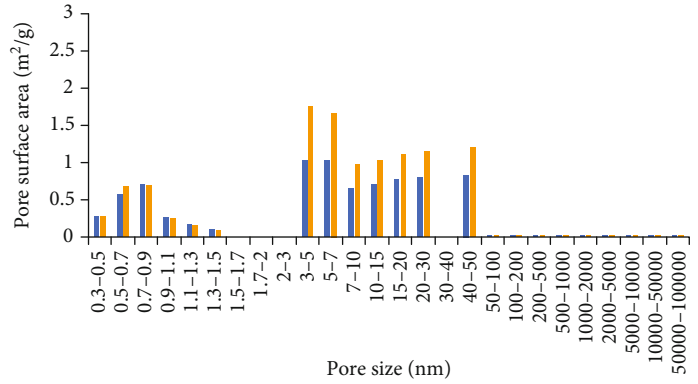

(j) 2555.65 m, organic-rich clayey shale

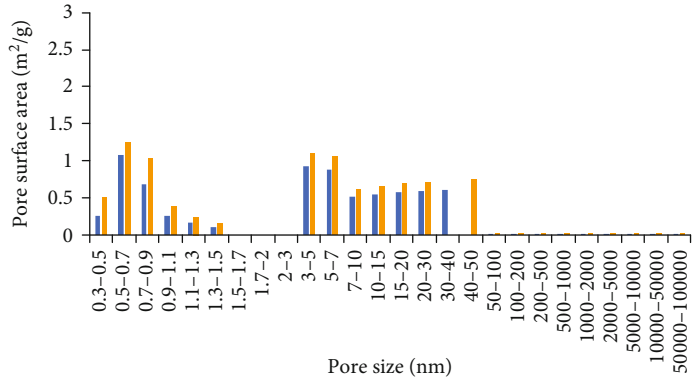

(k) 2573.32 m, organic-rich mixed shale

Figure 5: Continued.

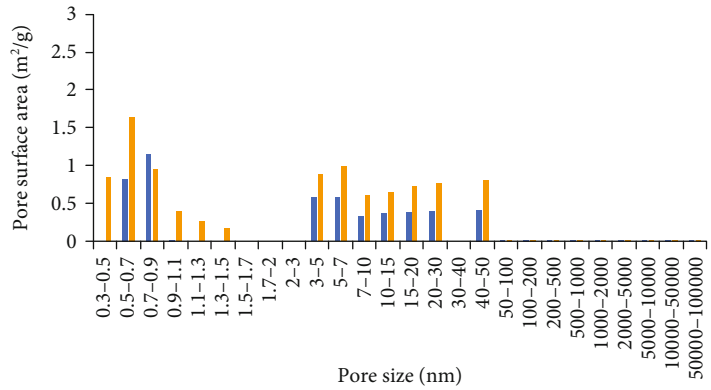

(l) 2576.98 m, organic-bearing clayey shale

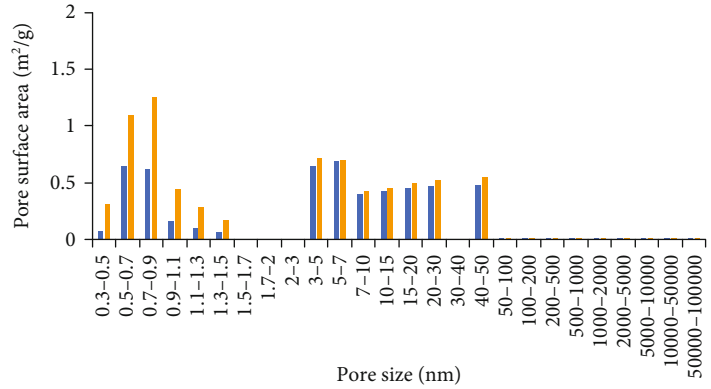

(m) 2579.45 m, organic-bearing clayey shale

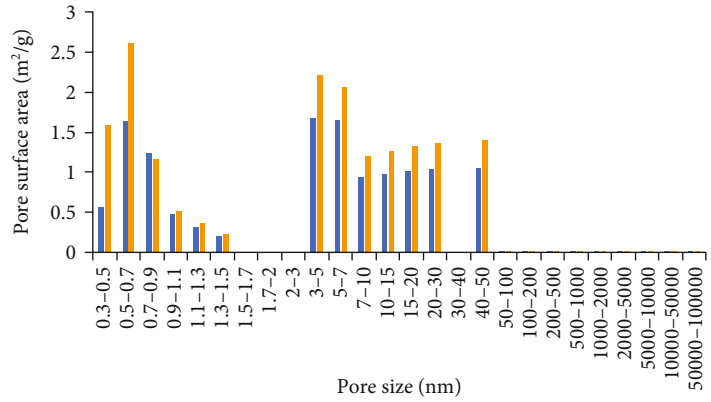

(n) 2589.7 m, organic-bearing clayey shale

Figure 5: Pore surface area features based on the joint characterization for full-scale pore size of different shale samples in TY1 well. Blue: pore surface area data of shale samples before the extraction of shale oil; Yellow: pore surface area data of shale samples after the extraction of shale oil.

shale oil was extracted. Thereinto, the organic-rich mixed and clayey mudstones have the highest pore volume of about 0.03 ml/g, which is followed by the value of about 0.025 ml/g in the fine sandstone; the organic-bearing clayey mudstone has a relatively low value of about 0.02 ml/g; and the organic-bearing mixed mudstone's pore volume is the lowest, showing a value of about 0.013 ml/g. In all types of lithofacies, the pore volume is predominantly provided by macropores (50% ~60%) and then by mesopores (about 40%).

By calculating the difference of the pore volume before and after extraction, the volume of pores where the free shale oil occurs can be obtained. As shown in Figure 6(a), the free shale oil contained in organic-rich clayey shale occupies the largest pore volume of about 0.01 ml/g, which is followed by the value of about 0.008 ml/g in organic-rich mixed shale and organic-bearing clayey shale; this oil contained in fine sandstone approximately occupies a pore volume of 0.005 ml/g; and it occupies the smallest pore volume of about 0.004 ml/g in organic-bearing mixed shale.

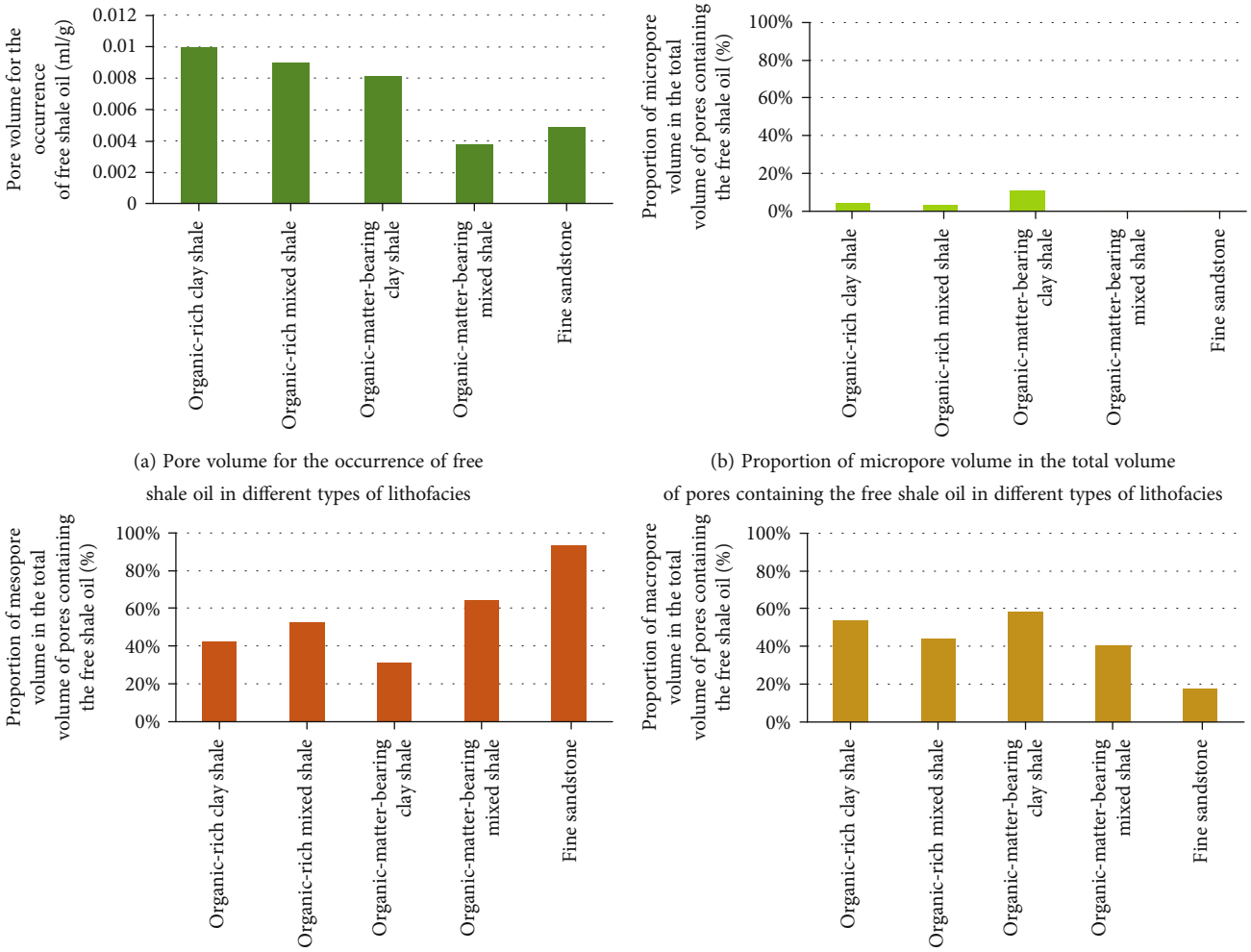

(a) Pore volume for the occurrence of free shale oil in different types of lithofacies

(b) Proportion of micropore volume in the total volume of pores containing the free shale oil in different types of lithofacies

(c) Proportion of mesopore volume in the total volume of pores containing the free shale oil in different types of lithofacies

(d) Proportion of macropore volume in the total volume of pores containing the free shale oil in different types of lithofacies

Figure 6: Pore volume characteristics for the occurrence of free shale oil in different types of lithofacies in TY1 well.

The main contributing pore types to the pore volume of the oil-bearing pores in the free state shale differ between the petrographic phases. According to Figures 6(b)–6(d), the free shale oil contained in organic-rich and organic-bearing clayey shales mainly occurs in macropores, which are followed by mesopores; that contained in organic-rich and organic-bearing mixed shales occurs mainly in mesopores, followed by macropores; and that contained in the fine sandstone primarily occurs in mesopores.

4.2.2. Pore Surface Area Characteristics for the Occurrence of Shale Oil. Similar to the pore volume, the analysis on the pore surface area characteristics of rock reservoirs also adopted the experimental data after the shale oil was extracted. The organic-rich clayey mudstone shows the highest pore surface area of about 12 m^2/g; the organic-rich mixed mudstone, organic-bearing clayey mudstone, and fine sandstone have a value of about 10 m^2/g; and the organic-bearing mixed mudstone shows the lowest value of 6.5 m^2/g. In all types of lithofacies, the pore surface area is primarily provided by mesopores (60%~90%) and then by micropores (5%~40%).

The difference of pore surface area before and after extraction helps to determine the surface area of pores where the absorbed shale oil occurs. As shown in Figure 7(a), the absorbed shale oil contained in organic-rich clayey shale occupies the largest pore surface area of over 4 m^2/g, and the values are similar in organic-rich mixed shale, organic-bearing clayey shale, organic-bearing mixed shale, and fine sandstone, fluctuating around 3 m^2/g.

Similarly, the pore surface area for the occurrence of shale oil in various types of lithofacies is provided by different pore types. According to Figures 7(b)–7(d), the absorbed shale oil contained in organic-bearing mixed shale and fine sandstone all occurs in mesopores; that contained in organic-rich clayey and mixed shales primarily occurs in mesopores, which are followed by micropores; and that contained in organic-bearing clayey shale mainly occurs in micropores, which are followed by mesopores.

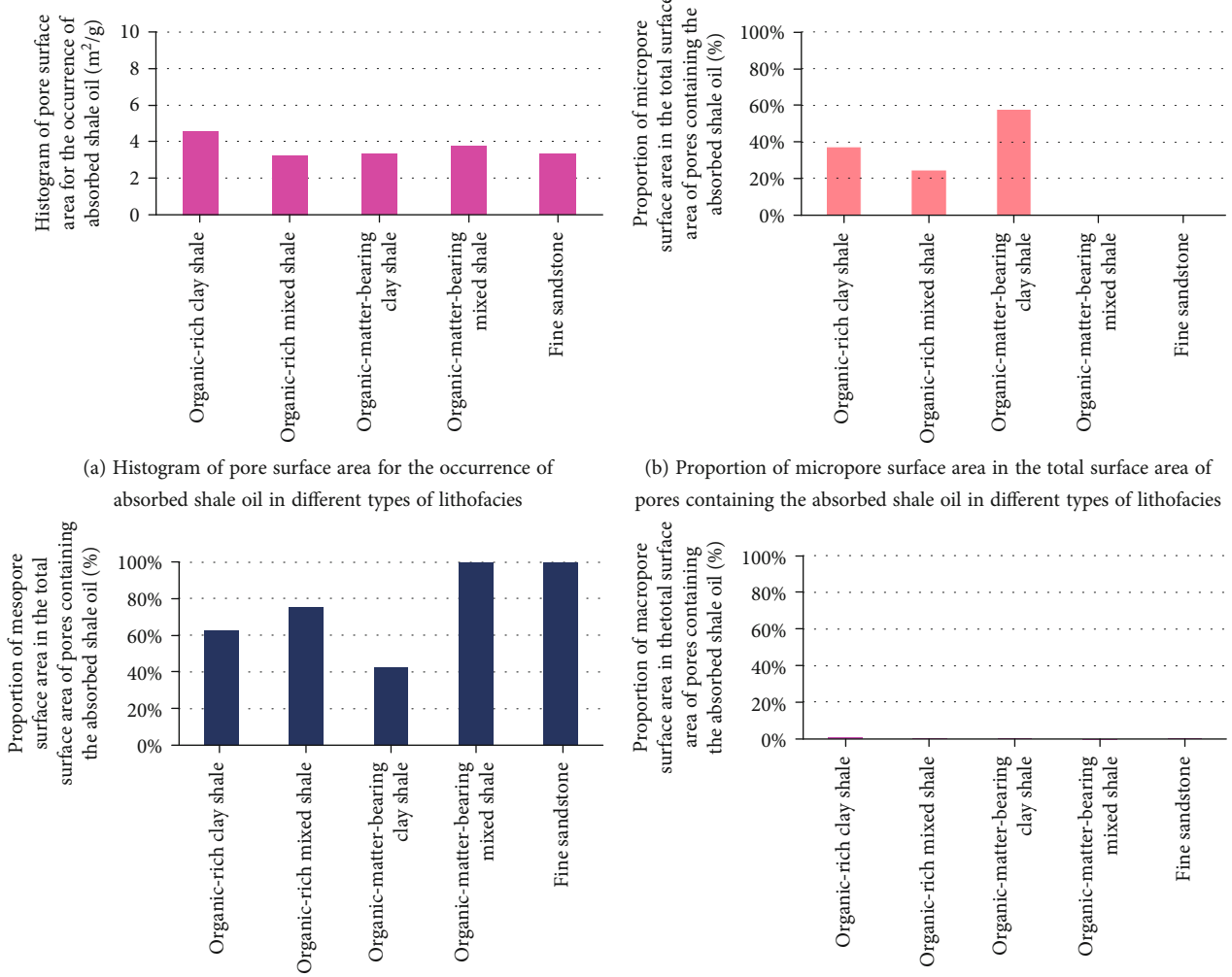

(a) Histogram of pore surface area for the occurrence of absorbed shale oil in different types of lithofacies

(b) Proportion of micropore surface area in the total surface area of pores containing the absorbed shale oil in different types of lithofacies

(c) Proportion of mesopore surface area in the total surface area of pores containing the absorbed shale oil in different types of lithofacies

(d) Proportion of macropore surface area in the total surface area of pores containing the absorbed shale oil in different types of lithofacies

Figure 7: Pore surface area characteristics for the occurrence of absorbed shale oil in different types of lithofacies in TY1 well.

5. Conclusions

In this paper, the rock cores are sampled from the Middle Jurassic Lianggaoshan Formation in southeastern Sichuan Basin of the Upper Yangtze area and are studied based on their TOC content, mineral composition, and shale lithofacies. Meanwhile, the experiments on CO_2 and N_2 adsorptions and high-pressure mercury injection are carried out before and after the shale oil is extracted by wash oil to compare the quantitative characterizations for the full-scale pore size and structure of samples before and after such extraction, thus obtaining the pore space characteristics for shale oil occurrence in different types of lithofacies. The following conclusions have been drawn.

(1) The characteristics of reservoirs vary significantly in different types of lithofacies. The organic-rich mixed and clayey mudstones, with the highest TOC content and the largest pore volume and surface area, provide abundant space for the occurrence of shale oil. Among them, macropores and mesopores contribute to the pore volume and surface area, respectively. In these two types of lithofacies, the free shale oil occupies the most reservoir space and predominantly occurs in macropores and mesopores; and the absorbed one occupies the largest reservoir space and primarily occurs in mesopores

(2) The organic-bearing clayey mudstone, with higher TOC content and larger pore volume and surface area, provides a certain space for the occurrence of shale oil. Notably, the pore volume and surface area originate from macropores and mesopores, respectively. In these lithofacies, the free shale oil occupies a larger space and mainly occurs in macropores, followed by mesopores, and the absorbed one also occupies a larger space and primarily occurs in micropores and then the mesopores

(3) The organic-bearing mixed mudstone has moderate TOC content and smaller pore volume and surface area, offering certain space for shale oil occurrence. Its pore volume and surface area are provided by macropores and mesopores, respectively. In this lithofacies, the free shale oil occupies a smaller reservoir space and mostly occurs in mesopores and then the macropores, and the absorbed one occupies a larger reservoir space and all occurs in mesopores

(4) The fine sandstone has a larger pore volume and surface area, which originate from macropores and mesopores, respectively, providing great space for the occurrence of shale oil. In these lithofacies, the free shale oil occupies a smaller reservoir space and mostly occurs in mesopores, and the absorbed one occupies a smaller reservoir space and all occurs in mesopores

Data Availability

Some of the data are contained in a published source cited in the references. All the data in this article are accessible to the readers.

Conflicts of Interest

The authors declare that they have no conflicts of interest.

Acknowledgments

This study was supported by the open funds from the National Natural Science Foundation of China (No. 42102192, No. 42130803, and No. 42072174); the State Key Laboratory of Shale Oil and Gas Enrichment Mechanisms and Effective Development (G5800-20-ZS-KFGY012); the Open Fund of Key Laboratory of Tectonics and Petroleum Resources (China University of Geosciences), Ministry of Education, Wuhan (TPR-2020-07); the Open Funds from the State Key Laboratory of Petroleum Resources and Prospecting (PRP/open-2107); and the Science and Technology Cooperation Project of the CNPC-SWPU Innovation Alliance.

References

[1] J. B. Curtis, "Fractured shale-gas systems," *AAPG Bulletin*, vol. 86, no. 11, pp. 1921–1938, 2002.

[2] X. Guo, Y. Li, T. Borjigen et al., "Hydrocarbon generation and storage mechanisms of deep-water shelf shales of Ordovician Wufeng Formation-Silurian Longmaxi Formation in Sichuan Basin, China," *Petroleum Exploration and Development*, vol. 47, no. 1, pp. 204–213, 2020.

[3] Z. He, S. Li, H. Nie, Y. Yuan, and H. Wang, "The shale gas "sweet window": "the cracked and unbroken" state of shale and its depth range," *Marine and Petroleum Geology*, vol. 101, no. 101, pp. 334–342, 2019.

[4] R. Wang, Z. Hu, L. Dong et al., "Advancement and trends of shale gas reservoir characterization and evaluation," *Oil & Gas Geology*, vol. 42, no. 1, pp. 54–65, 2021.

[5] R. Wang, H. Nie, Z. Hu, G. Liu, B. Xi, and W. Liu, "Controlling effect of pressure evolution on shale gas reservoirs: a case study of the Wufeng–Longmaxi Formation in the Sichuan Basin," *Natural Gas Industry*, vol. 40, no. 10, pp. 1–11, 2020.

[6] R. Wang, Z. Hu, S. Long et al., "Differential characteristics of the upper Ordovician-lower Silurian Wufeng-Longmaxi shale reservoir and its implications for exploration and development of shale gas in/around the Sichuan basin," *Acta Geologica Sinica-English Edition*, vol. 93, no. 3, pp. 520–535, 2019.

[7] X. Guo, D. Hu, Y. Li, Z. Wei, X. Wei, and Z. Liu, "Geological factors controlling shale gas enrichment and high production in Fuling shale gas field," *Petroleum Exploration and Development*, vol. 44, no. 4, pp. 513–523, 2017.

[8] Z. O. Caineng, P. A. Songqi, J. I. Zhenhua et al., "Shale oil and gas revolution and its impact," *Acta Petrolei Sinica*, vol. 41, no. 1, pp. 1–12, 2020.

[9] H. U.. Suyun, Z. H. A. O. Wenzhi, Y. A. N. G. Zhi et al., "Development potential and technical strategy of continental shale oil in China," *Petroleum Exploration and Development*, vol. 47, no. 4, pp. 877–887, 2020.

[10] K. Zhang, Y. Song, C. Jia et al., "Vertical sealing mechanism of shale and its roof and floor and effect on shale gas accumulation, a case study of marine shale in Sichuan basin, the upper Yangtze area," *Journal of Petroleum Science and Engineering*, vol. 175, no. 2019, pp. 743–754, 2019.

[11] K. Zhang, C. Jia, Y. Song et al., "Analysis of lower Cambrian shale gas composition, source and accumulation pattern in different tectonic backgrounds: a case study of Weiyuan block in the upper Yangtze region and Xiuwu Basin in the lower Yangtze region," *Fuel*, vol. 263, no. 2020, p. 115978, 2020.

[12] C. Zou, D. Dong, Y. Wang et al., "Shale gas in China: characteristics, challenges and prospects (II)," *Petroleum Exploration and Development*, vol. 43, no. 2, pp. 182–196, 2016.

[13] C. Zou, D. Dong, Y. Wang et al., "Shale gas in China: characteristics, challenges and prospects (I)," *Petroleum Exploration and Development*, vol. 42, no. 6, pp. 753–767, 2015.

[14] C. Zou, Q. Zhao, D. Dong et al., "Geological characteristics, main challenges and future prospect of shale gas," *Journal of Natural Gas Geoscience*, vol. 2, no. 5-6, pp. 273–288, 2017.

[15] T. Li, Z. Jiang, C. Xu et al., "Shale micro–nano pore structure characteristics in the lower third member of the continental Shahejie Formation, Zhanhua Sag," *Petroleum Science Bulletin*, vol. 2017, no. 4, pp. 445–456, 2017.

[16] S. Su, Z. Jiang, X. Shan et al., "Effect of lithofacies on shale reservoir and hydrocarbon bearing capacity in the Shahejie Formation, Zhanhua Sag, eastern China," *Journal of Petroleum Science and Engineering*, vol. 174, no. 174, pp. 1303–1308, 2019.

[17] C. Ning, Z. Ma, Z. Jiang et al., "Effect of shale reservoir characteristics on shale oil movability in the lower third member of the Shahejie Formation, Zhanhua Sag," *Acta Geologica Sinica - English Edition*, vol. 94, no. 2, pp. 352–363, 2020.

[18] S. Su, Z. Jiang, S. Xuanlong et al., "The effects of shale pore structure and mineral components on shale oil accumulation in the Zhanhua Sag, Jiyang Depression, Bohai Bay Basin, China," *Journal of Petroleum Science and Engineering*, vol. 165, no. 165, pp. 365–374, 2018.

[19] K. Zhang, Z. Jiang, L. Yin et al., "Controlling functions of hydrothermal activity to shale gas content-taking lower Cambrian in Xiuwu Basin as an example," *Marine and Petroleum Geology*, vol. 85, no. 2017, pp. 177–193, 2017.

[20] Z. C. Wang, W. Z. Zhao, Z. Y. Li, X. F. Jiang, and J. Li, "Role of basement faults in gas accumulation of Xujiahe Formation,

Sichuan Basin," *Petroleum Exploration and Development*, vol. 35, no. 5, pp. 541–547, 2008.

[21] Z. Juan, J. Tao, L. Xuesong, W. Tengqiang, G. Ruiying, and B. Rong, "Evaluation on exploration potentials of lower Jurassic reservoirs in eastern Sichuan Basin," *China Petroleum Exploration*, vol. 23, no. 4, 2018.

[22] K. Zhang, J. Peng, W. Liu et al., "The role of deep geofluids in the enrichment of sedimentary organic matter: a case study of the late Ordovician-early Silurian in the upper Yangtze region and early Cambrian in the lower Yangtze region, South China," *Geofluids*, vol. 2020, Article ID 8868638, 12 pages, 2020.

[23] C. Li, D. He, G. Lu, K. Wen, A. Simon, and Y. Sun, "Multiple thrust detachments and their implications for hydrocarbon accumulation in the northeastern Sichuan Basin, southwestern China," *AAPG Bulletin*, vol. 105, no. 2, pp. 357–390, 2021.

[24] K. Su, J. Lu, G. Zhang et al., "Origin of natural gas in Jurassic Da'anzhai Member in the western part of central Sichuan Basin, China," *Journal of Petroleum Science and Engineering*, vol. 167, no. 167, pp. 890–899, 2018.

[25] Y. Qing, Z. Lü, J. Wu et al., "Formation mechanisms of calcite cements in tight sandstones of the Jurassic Lianggaoshan Formation, northeastern Central Sichuan Basin," *Australian Journal of Earth Sciences*, vol. 66, no. 5, pp. 723–740, 2019.

[26] Z. Pang, S. Tao, Q. Zhang et al., "Enrichment factors and sweep spot evaluation of Jurassic tight oil in central Sichuan Basin, SW China," *Petroleum Research,*, vol. 4, no. 4, pp. 334–347, 2019.

[27] K. Zhang, Y. Song, S. Jiang et al., "Mechanism analysis of organic matter enrichment in different sedimentary backgrounds: a case study of the lower Cambrian and the upper Ordovician-lower Silurian, in Yangtze region," *Marine and Petroleum Geology*, vol. 99, no. 2019, pp. 488–497, 2019.

[28] X. Wang, S. He, X. Guo, B. Zhang, and X. Chen, "The resource evaluation of Jurassic shale in north Fuling area, eastern Sichuan Basin, China," *Energy & Fuels*, vol. 32, no. 2, pp. 1213–1222, 2018.

[29] C. Zou, S. Tao, Y. Fan, and X. Gao, "Characteristics of hydrocarbon accumulation and distribution of tight oil in China: an example of Jurassic tight oil in Sichuan Basin," *AAPG Search and Discovery*, vol. 2012, article 10386, pp. 1–6, 2012.

[30] J. Li, S. Z. Tao, Z. C. Wang, C. N. Zou, X. H. Gao, and S. Q. Wang, "Characteristics of Jurassic petroleum geology and main factors of hydrocarbon accumulation in NE Sichuan Basin," *Natural Gas Geoscience*, vol. 5, 2010.

[31] X. Lu, M. Li, X. Wang et al., "Distribution and geochemical significance of rearranged hopanes in Jurassic source rocks and related oils in the center of the Sichuan Basin, China," *ACS Omega*, vol. 6, no. 21, pp. 13588–13600, 2021.

[32] Z. Liu, G. Liu, Z. Hu et al., "Lithofacies types and assemblage features of continental shale strata and their implications for shale gas exploration: a case study of the middle and lower Jurassic strata in the Sichuan Basin," *Natural Gas Industry B*, vol. 7, no. 4, pp. 358–369, 2020.

[33] T. Li, Z. Jiang, P. Su et al., "Effect of laminae development on pore structure in the lower third member of the Shahejie shale, Zhanhua sag, eastern China," *Interpretation*, vol. 8, no. 1, pp. T103–T114, 2020.

[34] H. Guo, S. Liu, J. He, P. Zhu, and Q.-L. Zhang, "Hydrocarbon pooling conditions of the Jurassic Lianggaoshan Formation in Guangan area, central Sichuan Basin," *Natural Gas Industry*, vol. 28, no. 4, 2008.

[35] T. Li, Z. Jiang, C. Xu et al., "Effect of pore structure on shale oil accumulation in the lower third member of the Shahejie formation, Zhanhua sag, eastern China: evidence from gas adsorption and nuclear magnetic resonance," *Marine and Petroleum Geology*, vol. 88, no. 88, pp. 932–949, 2017.

[36] P. Wang, Z. Jiang, W. Ji et al., "Heterogeneity of intergranular, intraparticle and organic pores in Longmaxi shale in Sichuan Basin, South China: evidence from SEM digital images and fractal and multifractal geometries," *Marine and Petroleum Geology*, vol. 72, no. 72, pp. 122–138, 2016.

[37] W. Ji, Y. Song, Z. Jiang, X. Wang, Y. Bai, and J. Xing, "Geological controls and estimation algorithms of lacustrine shale gas adsorption capacity: a case study of the Triassic strata in the southeastern Ordos Basin, China," *International Journal of Coal Geology*, vol. 134-135, pp. 61–73, 2014.

[38] P. Wang, Z. Jiang, P. Li, C. Jin, X. Li, and P. Huang, "Organic matter pores and evolution characteristics of shales in the lower Silurian Longmaxi Formation and the lower Cambrian Niutitang Formation in periphery of Chongqing," *Natural Gas Geoscience*, vol. 29, no. 7, pp. 997–1008, 2018.

[39] X. Tang, Z. Jiang, S. Jiang, L. Cheng, and Y. Zhang, "Characteristics and origin of in-situ gas desorption of the Cambrian Shuijingtuo Formation shale gas reservoir in the Sichuan Basin, China," *Fuel*, vol. 187, no. 187, pp. 285–295, 2017.

[40] P. Wang, Z. Jiang, L. Chen et al., "Pore structure characterization for the Longmaxi and Niutitang shales in the upper Yangtze Platform, South China: evidence from focused ion beam-He ion microscopy, nano-computerized tomography and gas adsorption analysis," *Marine and Petroleum Geology*, vol. 77, no. 77, pp. 1323–1337, 2016.

[41] W. Ji, Y. Song, Z. Jiang et al., "Micro-nano pore structure characteristics and its control factors of shale in Longmaxi Formation, southeastern Sichuan Basin," *Acta Petrolei Sinica*, vol. 37, no. 2, pp. 182–195, 2016.

[42] F. Yang, S. Xu, F. Hao et al., "Petrophysical characteristics of shales with different lithofacies in Jiaoshiba area, Sichuan Basin, China: implications for shale gas accumulation mechanism," *Marine and Petroleum Geology*, vol. 109, pp. 394–407, 2019.

[43] W. Ji, Y. Song, Z. Jiang et al., "Fractal characteristics of nanopores in the lower Silurian Longmaxi shales from the upper Yangtze Platform, South China," *Marine and Petroleum Geology*, vol. 78, pp. 88–98, 2016.

[44] T. Li, Z. Jiang, Z. Li et al., "Continental shale pore structure characteristics and their controlling factors: a case study from the lower third member of the Shahejie Formation, Zhanhua Sag, Eastern China," *Journal of Natural Gas Science and Engineering*, vol. 45, no. 45, pp. 670–692, 2017.

[45] W. Ji, Y. Song, Z. Jiang et al., "Estimation of marine shale methane adsorption capacity based on experimental investigations of lower Silurian Longmaxi formation in the upper Yangtze Platform, South China," *Marine and Petroleum Geology*, vol. 68, pp. 94–106, 2015.

[46] F. Yang, Z. Ning, Q. Wang, R. Zhang, and B. M. Krooss, "Pore structure characteristics of lower Silurian shales in the southern Sichuan Basin, China: insights to pore development and gas storage mechanism," *International Journal of Coal Geology*, vol. 156, pp. 12–24, 2016.

[47] F. Yang, B. Hu, S. Xu, Q. Meng, and B. M. Krooss, "Thermodynamic characteristic of methane sorption on shales from oil, gas, and condensate windows," *Energy & Fuels*, vol. 32, no. 10, pp. 10443–10456, 2018.

[48] F. Yang, B. Lyu, and S. Xu, "Water sorption and transport in shales: an experimental and simulation study," *Water Resources Research*, vol. 57, no. 2, 2021.

[49] K. Zhang, Y. Song, S. Jiang et al., "Shale gas accumulation mechanism in a syncline setting based on multiple geological factors: an example of southern Sichuan and the Xiuwu Basin in the Yangtze region," *Fuel*, vol. 241, no. 2019, pp. 468–476, 2019.

[50] K. Zhang, J. Peng, X. Wang et al., "Effect of organic maturity on shale gas genesis and pores development: a case study on marine shale in the upper Yangtze region, South China," *Open Geosciences*, vol. 12, no. 1, pp. 1617–1629, 2020.

[51] B. Liu, S. He, L. Meng, X. Fu, L. Gong, and H. Wang, "Sealing mechanisms in volcanic faulted reservoirs in Xujiaweizi extension, northern Songliao Basin, northeastern China," *AAPG bulletin*, vol. 105, no. 8, pp. 1721–1743, 2021.

[52] B. Liu, J. Sun, Y. Zhang et al., "Reservoir space and enrichment model of shale oil in the first member of Cretaceous Qingshankou Formation in the Changling sag, southern Songliao Basin, NE China," *Petroleum Exploration and Development*, vol. 48, no. 3, pp. 608–624, 2021.

[53] H. Huang, R. Li, Z. Jiang, J. Li, and L. Chen, "Investigation of variation in shale gas adsorption capacity with burial depth: insights from the adsorption potential theory," *Journal of natural gas science and engineering*, vol. 73, article 103043, 2020.

[54] Z. Gao and Q. Hu, "Pore structure and spontaneous imbibition characteristics of marine and continental shales in China," *AAPG Bulletin*, vol. 102, no. 10, pp. 1941–1961, 2018.

[55] Z. Gao, Z. Liang, Qinhong Hu, Z. Jiang, and Q. Xuan, "A new and integrated imaging and compositional method to investigate the contributions of organic matter and inorganic minerals to the pore spaces of lacustrine shale in China," *Marine and Petroleum Geology*, vol. 127, article 104962, 2021.

[56] P. Wang, Z. Jiang, L. Yin et al., "Lithofacies classification and its effect on pore structure of the Cambrian marine shale in the upper Yangtze Platform, South China: evidence from FE-SEM and gas adsorption analysis," *Journal of Petroleum Science and Engineering*, vol. 156, no. 2017, pp. 307–321, 2017.

[57] K. Zhang, Z. Li, S. Jiang et al., "Comparative analysis of the siliceous source and organic matter enrichment mechanism of the upper Ordovician–lower Silurian shale in the upper-lower Yangtze area," *Minerals*, vol. 8, no. 7, p. 283, 2018.

[58] K. Zhang, Z. Jiang, X. Xie et al., "Lateral percolation and its effect on shale gas accumulation on the basis of complex tectonic background," *Geofluids*, vol. 2018, Article ID 5195469, 11 pages, 2018.

[59] X. Tang, Z. Jiang, Y. Song et al., "Advances on the Mechanism of Reservoir Forming and Gas Accumulation of the Longmaxi Formation Shale in Sichuan Basin, China," *Energy & Fuels*, vol. 35, no. 5, pp. 3972–3988, 2021.

[60] K. Zhang, Y. Song, S. Jiang et al., "Accumulation mechanism of marine shale gas reservoir in anticlines: a case study of the southern Sichuan Basin and Xiuwu Basin in the Yangtze region," *Geofluids*, vol. 2019, Article ID 5274327, 14 pages, 2019.